Comprehensive Cost based Energy Management Strategy of Electric Vehicles with Hybrid Energy Storage System

Juanying Zhou[1,2*] , Jianyou Zhao[1] , Lufeng Wang[3]

1.School of Automobile, Chang'an University, Xi'an Shaanxi, 710064, China
2.College of Automotive Engineering and General Aviation, Shaanxi Vocatinal&Technical College, Xi'an Shaanxi 710038, China
3.College of Automobile, Shaanxi College of Communication Technology, Xi'an Shaanxi 710018, China

CA Juanying Zhou email: 2015221010080@stu.scu.edu.cn
Jianyou Zhao email: 372970312@qq.com
Lufeng Wang email: 250135620@qq.com

ABSTRACT In order to improve the economy of electric vehicles with a hybrid energy storage system (HESS) composed of power batteries and ultracapacitors, this work uses the minimization and weighted sum of battery capacity loss and energy consumption under driving cycles as objective functions. Dynamic programming is employed to determine the objective function values under different weight coefficients, obtain comprehensive cost composed of battery aging and power consumption costs, and elucidate the corresponding hybrid power distribution relationship. Based on the overall optimization results, particle swarm optimization is then used to optimize the membership parameters of fuzzy logic, and a real-time fuzzy energy management strategy is developed. Taking the WLTP driving cycle and a synthesis driving cycle derived from NEDC, WLTP, and UDDS as examples, the real-time fuzzy energy management strategy, fuzzy control strategies, and a strategy based on dynamic programming are evaluated, and the strategy proposed in this work is compared with the fuzzy control and based on dynamic programming strategies. The results show that, compared with the fuzzy control strategy, the proposed energy management strategy reduces the battery capacity loss by 24.374% and 22.181%, the system energy consumption increases by 4.900% and 4.824%, and the comprehensive cost is reduced by 9.953% and 9.292%, respectively, for the WLTP and synthesis driving cycles. Compared with the strategy based on dynamic programming, the battery capacity loss is reduced by 24.374% under the WLTP cycle and increased by 2.043% under the synthesis cycle. For these two cycles, the respective system energy consumption are increased by 5.216% and 10.882%, and the respective comprehensive costs are increased by 1.759% and 3.790%. These results demonstrate the effectiveness of the proposed energy management strategy in improving the economy of electric vehicles that use HESS.

INDEX TERMS automobile engineering, hybrid energy storage, energy management, fuzzy control strategy.

1. INTRODUCTION

Relative to gasoline and diesel powered vehicles, electric vehicles (EVs) have the advantages of energy saving, emission reduction, low noise, and simple power system structure, advantages that give them a prominent place in sustainable transportation. EVs that use a hybrid energy storage system (HESS) [1, 2] composed of an ultracapacitor and power batteries combine the advantages of these two forms of energy storage. HESS can protect the power battery, improve vehicle economy, and help to overcome mileage anxiety [3-4].

HESS's power battery and ultracapacitor act in tandem to store energy and provide power as needed. An energy management strategy (EMS) can optimize system efficiency and improve vehicle economy. Typical EMS include rule-based strategies [5-7] (such as logic rules and fuzzy logic [8-12]), intelligent algorithm-based strategies (such as convex optimization [13] and genetic algorithm [14]), and global optimization algorithms (such as dynamic programming [15]). Particle swarm optimization (PSO) has attracted more and more attention because of its simple mechanism, its relatively small number of parameters, and the advantages of integrating it with other algorithms to improve overall optimization performance [16].

The cost of the power battery accounts for a substantial portion of the total cost of the whole vehicle. In the design of EMS, the aging factor of the battery needs to be fully considered in order to prolong its service life and thereby improve the economy of the whole vehicle and the value of its entire life cycle [17]. In ref. [2], the optimization goals were to minimize the energy consumption of the composite power supply and the capacity loss of the battery pack, for which purpose dynamic programming was applied to match the parameters of the composite power supply. In ref. [8], including both the total cost and total quality of the composite energy storage system as parts of the optimization goal, a rule-based control strategy was formulated, and a composite fuzzy control strategy was proposed. In ref. [13], the optimization goal was the weighted sum of the initial cost and cost of the composite power supply, and convex optimization was used to optimize the power distribution. In ref. [14], a multi-part objective was established: minimizing both the replacement cost of the composite power supply and the average daily energy consumption. The optimization function uses a genetic algorithm to optimize the energy management strategy of the composite power supply. A rule-based energy management strategy was then presented on this basis. While the rule-based control strategy is simple, its optimization requires further improvement. Additionally, fuzzy control is suitable for time-varying systems and is robust, but its control strategy is based mainly on expert experience and is subjective. The use of optimization algorithms to optimize fuzzy controllers can more effectively adapt to changes in operating cycles [19-20]. The optimization problem’s convexity must be take into account when convex optimization is applied, which is difficult in practical application, while the genetic algorithm has a low convergence speed and can easily fall into a local minimum. Dynamic programming (DP) can achieve global optimization, but it is slow.

In view of the problems of poor optimization results, strong subjectivity, difficulty in actual use, and long calculation time of the above EMS, the work

reported here takes an electric vehicle with batteries and ultracapacitors as the research object. The weighted sum of battery capacity loss and energy consumption is minimized as the optimization goal, and dynamic programming is used to solve the objective function under different weight coefficients. The comprehensive cost composed of battery aging cost and energy consumption cost and the corresponding power distribution relationship between the power battery and the ultracapacitor are obtained. Based on these results, particle swarm optimization (PSO) is then applied to optimize fuzzy logic membership parameters, and a real-time fuzzy energy management strategy is developed.

2. STRUCTURE OF THE RESEARCH

The arrangement of this paper is shown in Fig. 1. Section 3 introduces configuration characteristics of the model electric vehicle system with batteries and ultracapacitors. In Section 4, the Wordwide Harmonized Light Vehicle Test (WLTP) driving cycle is selected as the research driving cycle, and a synthesis of New European Driving Cycle (NEDC), WLTP, and Urban Dynamometer Driving Schedule (UDDS) is selected as a verification driving cycle. In Section 5, the objective function that minimizes the weighted sum of the capacity loss and energy consumption of the power battery under cycling is constructed, and dynamic programming (DP) is used to solve the objective function value under different weight coefficients. In this section, comprehensive cost is introduced as a measure of the energy management strategy. It includes the purchase price of the battery pack and takes into account different electricity prices, assigned to the comprehensive cost with weight coefficients, as the independent variable under different electricity prices, and obtain the weight coefficient and the corresponding power distribution relationship when the comprehensive cost is the smallest. In Section 6, based on the above global optimization results, particle swarm optimization is used to optimize fuzzy logic membership parameters, and a real-time fuzzy energy management strategy is developed. Section 7 discusses the fuzzy strategy and fuzzy control based on particle swarm optimization in the WLTP and synthesis cycles. The proposed EMS, the fuzzy logic strategy, and the EMS based on DP are simulated and analyzed in this section, and the energy management strategy proposed in this paper is compared with the fuzzy control strategy and the EMS based on DP. Section 8 presents the conclusions and points to future work.

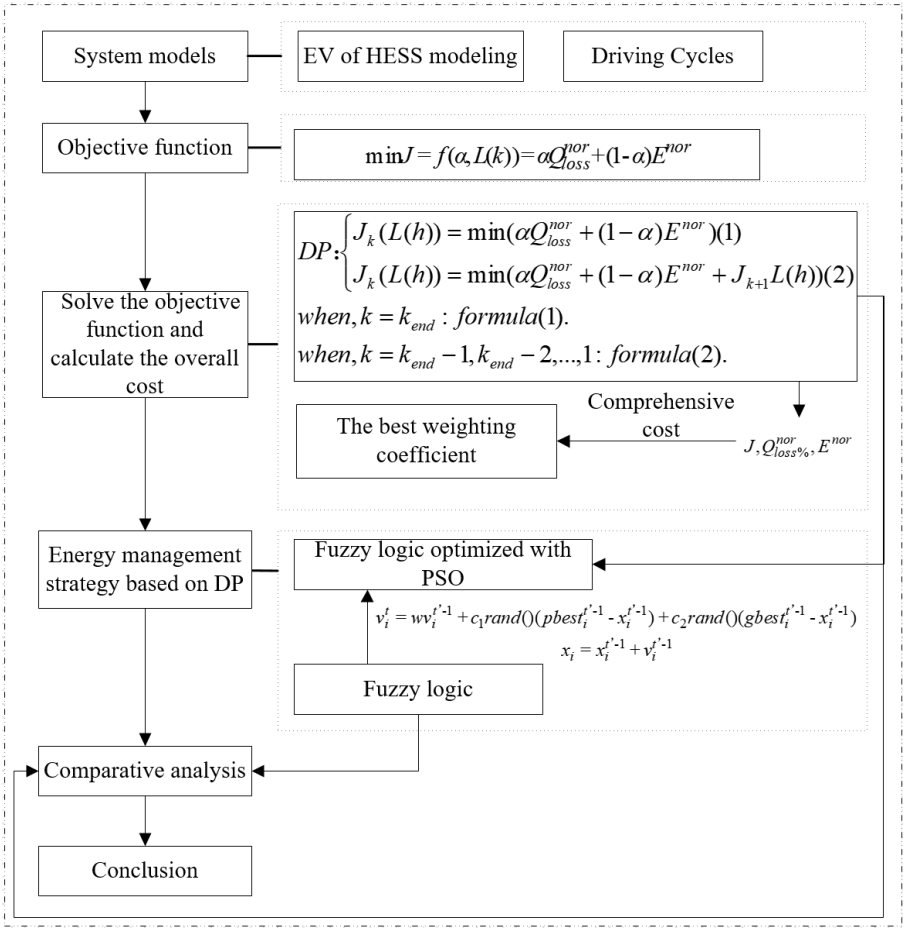

Figure 1. The arrangement of this paper.

3. COMPOSITE POWER ELECTRIC VEHICLE STRUCTURE AND PARAMETERS

3. 1. Structure of hybrid energy storage system in an electric vehicle

There are many types of HESS. In our version of HESS, the ultracapacitor is connected in series with DC-DC and connected in parallel with the battery pack to connect to the DC bus, providing the advantages of simple structure and convenient control. The structure is shown in Fig. 2. The energy management system (EMS) calculates the ultracapacitor output power and battery output power according to the collective state of charge of the battery (SOC_b), the state of charge of the ultracapacitor (SOC_u), and the power (P) [2].

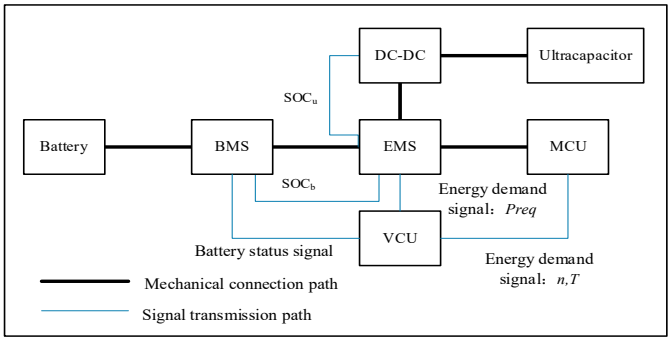

Figure 2. Structure of HESS.

3.2 Electric machine (EM)

A permanent magnet synchronous motor is used as the electric machine (EM) model. Its maximum speed is 8000 rpm, its maximum power is 105 kW, and its maximum torque is 180 N·m. The electric power of the drive motor can be expressed as a relationship between the motor output power and the motor efficiency:

$$P_{em} = \frac{T_m \cdot \omega_m}{9.55} \cdot \eta_m^z(T_m, \omega_m) \tag{1}$$

where P_{em} is the power of the EM, T_m is the torque, ω_m is the angular velocity, and η_m is the EM's efficiency, which is expressed as a function of the torque and rotational speed. In this paper, the calculation is carried out in the form of a look-up table. The functional relationship is shown in Fig. 3. In the figure, z is the index coefficient: when $z = -1$, the machine works as a motor; when z = 1, the machine works as a generator.

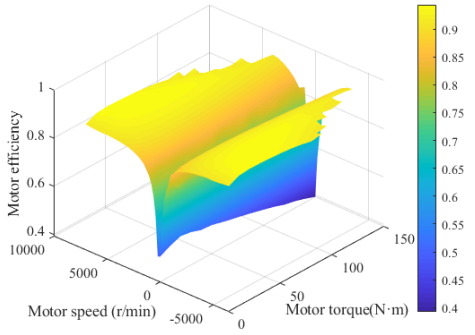

Figure 3. Model of motor efficiency.

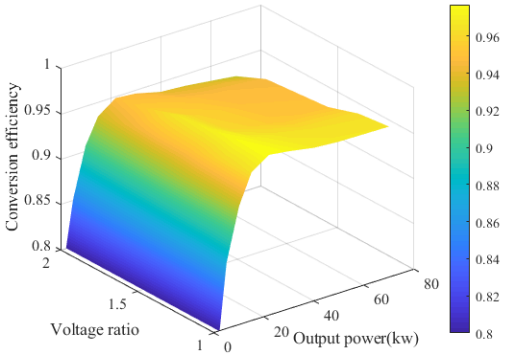

Figure 4. Efficiency of DC-DC.

3.3 Power of the DC bus

The power of the DC bus is defined by

$$\begin{cases} P_{dri} = P_b + P_u \eta_{DC-DC} \\ P_{re} = P_b + P_u / \eta_{DC-DC} \end{cases} \tag{2}$$

where P_{dri} is the driving power, P_b is the battery power, P_u is the ultracapacitor power,

P_{re} is the bus power in the energy feedback, and $\eta_{DC\text{-}DC}$ is the DC-DC conversion efficiency. The functional relationship is shown in Figure 4.

3.4 Ultracapacitor

Figure 5 shows the ultracapacitor model. The ultracapacitor has a nominal capacitance of 28 F and a rated voltage of 399 V. The ultracapacitor model is described by

$$U_u = U - I_u R_u \tag{3}$$

and the power of the ultracapacitor is given by

$$P_u = U_u I_u - I_u^2 R_u \tag{4}$$

where U_u is the output voltage of the ultracapacitor, U is the open-circuit voltage of the ultracapacitor, I_u is the current of the ultracapacitor (discharge is positive, charge is negative), and R_u is the capacitor equivalent internal resistance, as shown in Fig. 6.

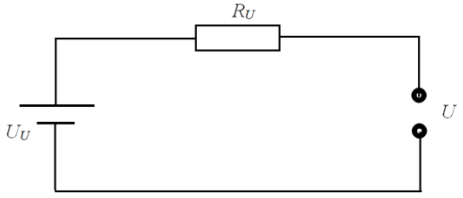

Figure 5. Ultracapacitor model.

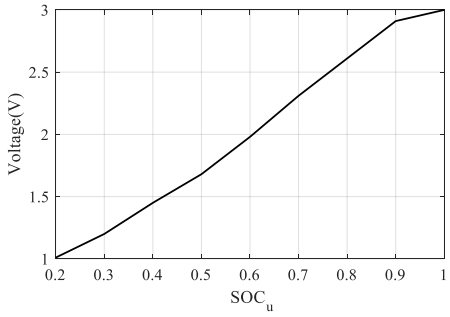

Figure 6. Resistance of the voltage and state of charge.

3.5 Battery

3.5.1 Battery circuit model

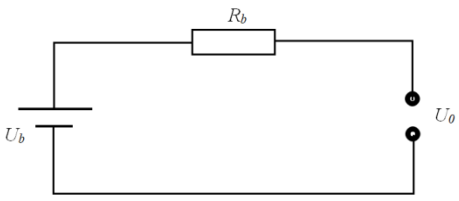

Figure 7. Model of the battery.

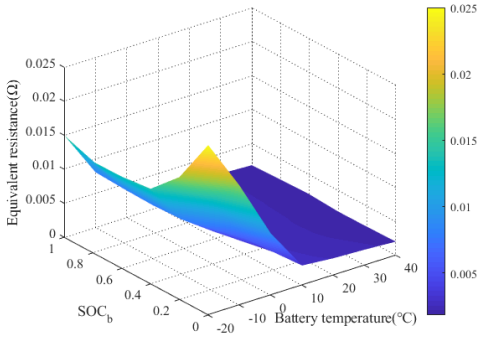

Figure 8. Resistance of the battery.

The nominal capacity of the power battery pack is 102 A·h, and the total rated voltage is 400 V. The battery model adopts the Rint-model of internal resistance voltage [17], as shown in Fig. 7. The battery model can be described by

$$U_b = U_0 - I_b R_b \tag{5}$$

The power of the battery is defined as

$$P_b = U_b I_b - I_b^2 R_b \tag{6}$$

where U_b is the battery voltage, U_0 is the open-circuit voltage of the battery, I_b is the battery current, and R_b is the internal resistance of the battery, which includes ohmic resistance, concentration polarization resistance, and charge transfer resistance. The relationship between battery internal resistance, SOC_b, and battery ambient temperature is shown in Fig. 8.

3.5.2 Battery thermal model

For the temperature rise of the power battery the Bernardi heat production model [21] is chosen. It can be defined as

$$\frac{dT}{dt} = \frac{R_b I_b^2}{m_b C_p} - \frac{T I_b}{m_b C_p} \frac{dE_0}{dT} \tag{7}$$

where dT/dt is the rate of change of the battery's kelvin temperature, m_b is the mass of the single battery, C_p is the equivalent kelvin specific heat capacity of the battery, T is the temperature of the battery, and dE_0/dT is temperature rise coefficient of the battery.

The ambient temperature of the battery is controlled by the thermal management system of the whole vehicle. In this study, referring to the thermal management system of the power battery of an EV model, the maximum working temperature of the power battery is set to 35 °C (308.15 K).

HESS parameter values are shown in Table 1.

Table 1. HESS parameter values

Parameter	Value
Series number of batteries	108
Parallel number of batteries	34
Series number of ultracapacitors	133
Parallel number of ultracapacitors	1

3.6 Vehicle longitudinal dynamics

The required power of the vehicle is based on the formula governing the longitudinal force of the vehicle. We employ backward simulation to solve the driving power required by the vehicle through the speed and acceleration of each cycle. The required power P_{req} can be written

$$P_{\mathrm{req}} = (Gf\cos\theta + AC_d\rho v^2 / 21.15 + \delta m\frac{dv}{dt} + G\sin\theta)v/(3600\eta_m^z) \tag{8}$$

where G is the weight of the vehicle, f is the rolling resistance, θ is the slope of the road, A is the windward area, C_d is the aerodynamic drag coefficient, ρ is the air density, v is the velocity of the vehicle, δ is the correction coefficient of the rotation mass, m is the gross mass of the vehicle, and η_T is the efficiency of the drive train.

The main parameters of the vehicle simulation model are provided in Table 2.

Table 2. Main parameters of the vehicle simulation model

Parameter	Value
Mass of the vehicle/kg	1400
Rolling resistance	0.01
Windward area/m^2	1.60
Aerodynamic drag coefficient	0.30
Air density/kg/m^3	1.18
Correction coefficient of the rotation mass	1.10
Efficiency of the drive train	0.95

4. DRIVING CYCLE SELECTION

The driving cycle describes the vehicle's speed over time. Driving cycles are the main benchmark for calibrating and optimizing various vehicle performance indicators.

We employ WLTP as the research driving cycle, where the average speed is 46.5 km/h and the maximum speed is 131.3 km/h. The WLTP driving cycle is divided into low-speed, medium-speed, high-speed, and extremely high-speed according to the average driving speed, as shown in Fig. 9.

Three different driving cycles (NEDC, UDDS, WLTP), including urban, suburban, and expressway, are randomly selected. In order to verify the universality of the optimization effect of the proposed energy management strategy, the representative speed range is combined with a new driving cycle, and the synthesized driving cycles are composed of low-speed NEDC and WLTP driving cycles, medium-speed UDDS and WLTP driving cycles, and high-speed NEDC and UDDS driving cycles [22], as shown in Fig. 10.

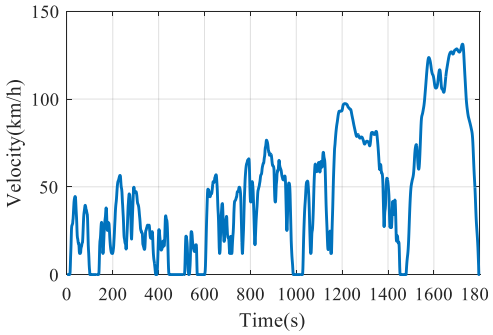

Figure 9. WLTP driving cycle.

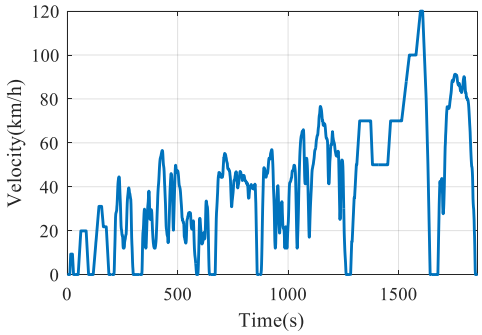

Figure 10. Synthesis driving cycle.

5. ENERGY MANAGEMENT STRATEGY BASED ON DYNAMIC PROGRAMING (DP-EMS)

5.1 Objective function construction

The energy management strategy of the vehicle composite power supply is one of the keys to improving vehicle performance. It seeks to balance battery life and energy consumption. Introducing the weight coefficient α, an objective function is constructed to minimize the weighted sum of the battery's capacity loss and energy consumption under driving cycles:

$$\min \quad J = f(\alpha, L(k)) = \alpha Q_{loss}^{nor} + (1-\alpha) E^{nor} \tag{9}$$

where J is the objective function, α is the weight coefficient (whose value ranges from 0 to 10), L is the sequence of control variables, Q_{loss}^{nor} is the capacity loss of the battery , and E^{nor} is the normalized cyclic energy consumption of HESS. Q_{loss}^{nor} and E^{nor} can be described as

$$\begin{cases} Q_{loss}^{nor} = \dfrac{Q_{loss} - Q_{loss}^{\min}}{Q_{loss}^{\max} - Q_{loss}^{\min}} \\ E^{nor} = \dfrac{E - E^{\min}}{E^{\max} - E^{\min}} \end{cases} \quad (10)$$

where

$$\begin{cases} Q_{loss} = B \cdot \exp\left(\dfrac{-31700 + 163.3 \cdot I_b}{R \cdot T}\right) \cdot AH^{0.57} \\ E = \int_{t_0}^{t_f} P_b(\tau) d\tau + \int_{t_0}^{t_f} P_u(\tau) d\tau \end{cases} \quad (11)$$

in which the superscripts *min* and *max* represent the minimum and maximum values of the variables they refer to, B is a preexponential factor, R is the gas constant, 8.314, T is the battery temperature expressed in kelvins, t_0 and t_f are the trip start and end times, AH is the Ah-throughput, described by Eq. (12) below, and σ is the severity factor which can be obtained empirically using Eq. (13) below:

$$AH = \int_{t_0}^{t_f} \sigma(I(\tau), T(\tau), SOC_b(\tau)) \cdot I(\tau) d\tau \quad (12)$$

$$\sigma\left(I(t), T(t), SOC_b(t)\right) = \left[\frac{(\beta \cdot SOC_b(t) + \gamma) \cdot \exp\left(\dfrac{-31700 + 163.3 \cdot I_b(t)}{R \cdot T(t)}\right)}{(\beta \cdot SOC_{nom} + \gamma) \cdot \exp\left(\dfrac{-31700 + 163.3 \cdot I_{nom}}{R \cdot T_{nom}}\right)} \right]^{\frac{1}{0.57}} \quad (13)$$

where t is the duration, β and γ are the fitting coefficients related to SOC_b. In this study, β = 1385.5 and γ = 4193.2, Additionally, SOC_{nom}, T_{nom}, and I_{nom} are, respectively, the battery SOC, temperature and current in nominal cycles. In this study, SOC_{nom} = 0.35, T_{nom} = 298.15 K, and I_{nom} = 0.35.

5.2 Dynamic programming

The core concept of dynamic programming (DP) is to transform a complex multi-stage globally optimal decision problem into a multi-stage local optimal problem and to obtain the optimal solution of each stage separately to ensure that the optimization problem achieves the globally optimal solution. According to the optimal control theory of dynamic programming [23-24], the discrete form of the dynamic

programming iterative format with the optimization objective function as the performance index is

when k=k_{end}

$$J_k(L(h)) = \min(\alpha Q_{loss}^{nor} + (1-\alpha)E^{nor}) \quad (14)$$

when k=k_{end}-1, k=k_{end}-2,...,1

$$J_k(L(h)) = \min(\alpha Q_{loss}^{nor} + (1-\alpha)E^{nor} + J_{k+1}(L(h))) \quad (15)$$

where J_k is the k stage (hth) objective function value. In this work, L∈[0:0.01:1].

α is substituted into Eq. (9) to solve the objective function value under different weight coefficients, as shown in Fig. 11.The capacity loss of the battery and the system cycle energy consumption are then obtained, as shown in Fig. 12.

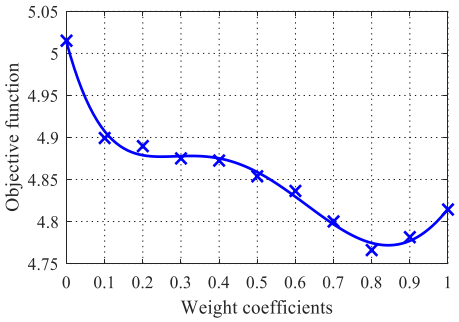

Figure 11. Optimal solution variable with different weight coefficients.

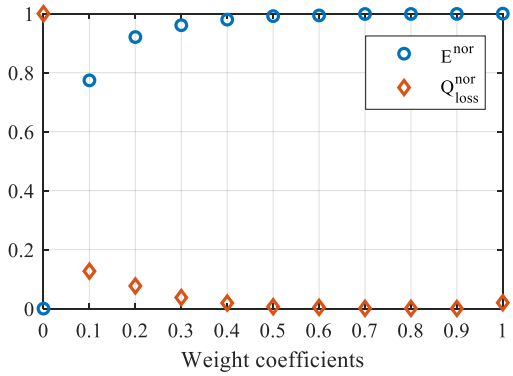

Figure 12. The value of battery loss and energy consumption with different weight coefficients.

When α = 0, the optimization goal is based completely on the system cycle energy consumption. At this point, the system cycle energy consumption is the least, the battery capacity loss is the greatest, and the composite power system is closest to the working state of a single battery.

When α = 1, the optimization goal is based completely on the battery life. The battery capacity loss is then the smallest and the system cycle energy consumption is the largest.

5.3 Solute optimal weight coefficient based on comprehensive cost

The comprehensive cost is the sum of battery aging cost and power consumption cost. The battery aging cost is the purchase cost of the battery pack shared by the loss of the battery capacity in the current trip. The energy consumption cost is the power consumption cost of the power battery and the output power of the ultracapacitor, which can be described as

$$F_c = C_{br} + C_e \tag{16}$$

where F_c is the comprehensive cost, C_{br} is the battery aging cost, and C_e is the energy consumption cost.

$$\begin{cases} C_{br} = \dfrac{P_{br} \cdot \int_{t_0}^{t_f} (\beta SOC_b(\tau) + \gamma) \cdot \exp(\dfrac{-31700 + 163.3 I_b(\tau)}{R \cdot T(\tau)}) \cdot AH(\tau)^{0.57} d\tau}{Q_{EOL\%}} \\ C_e = \dfrac{p_e \cdot \int_{t_0}^{t_f} (P_b(\tau) + P_u(\tau)) d\tau}{3.6 \times 10^6} \end{cases} \tag{17}$$

in which P_{br} is the battery pack acquisition cost (1000 yuan/(kw·h)), $Q_{EOL\%}$ is the capacity loss percentage when battery end of its life , and P_e is electricity price.

The cost of electricity consumption is related to the unit price of electricity. Taking Xi'an as an example: the price of commercial AC slow charging is 0.8 yuan/(kw·h), and the DC fast charging price ranges from 1.0 to 1.5 yuan/(kw·h). Substituting the battery capacity loss and system cycle energy consumption under different weight coefficients into Eqs. (16) and (17), the fitting formula is found to be

$$\begin{bmatrix} F_{c1} \\ F_{c2} \\ F_{c3} \end{bmatrix} = \begin{bmatrix} -171.2 & 655.2 & -1008.3 & 800.1 & -348.1 & 81.1 & -9.1 & 3.7 \\ -215.9 & 835.9 & -1308.9 & 1062.4 & -475.4 & 115 & -13.7 & 4.3 \\ -369.2 & 1434.8 & -2259 & 1847.9 & -836.5 & 206.2 & -25.4 & 5.8 \end{bmatrix} \cdot \begin{bmatrix} \alpha^7 \\ \alpha^6 \\ \vdots \\ 1 \end{bmatrix} \tag{18}$$

where F_{c1} is the comprehensive cost of AC slow charging with an electricity price of 0.8 yuan/(kw h); F_{c2} and F_{c3} are, respectively, the comprehensive costs with electricity prices of 1.0 and 1.5 yuan/(kw·h) for DC fast charging.

The comprehensive cost for several electricity prices can be determined, as shown in Fig. 13.

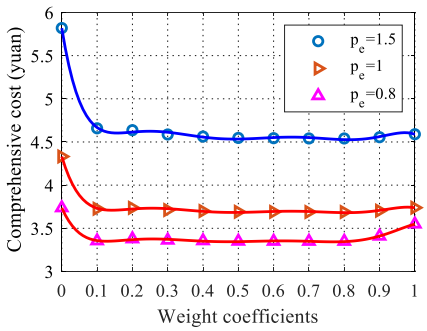

Figure 13. Comprehensive cost for different electric prices and weight coefficients.

This figure shows the combined cost of different electricity prices. Taking the AC slow charging price (P_{e1} = 0.8) as an example: When α = 0.78, the minimum comprehensive cost per cycle is 3.34 yuan. When the DC fast charging price P_{e2}=1.0 is taken as an example, and with α = 0.81, the minimum comprehensive cost per cycle is 3.68 yuan. When the fast charging price P_{e2} = 1.5, with α =0.83, is adopted, the minimum comprehensive cost per cycle is 4.53 yuan. The research object of this paper is commercial vehicles, which require high charging speed. Therefore, this study considers that the lowest comprehensive cost when the DC fast charging price price (P_{e1} = 1.5yuan/(kw·h)) and α = 0.83.

6. ENERGY MANAGEMENT STRATEGY OPTIMIZATION

The optimal energy management strategy obtained by DP cannot be applied in real time, but its optimization result can be used to evaluate the effect of the energy management strategy.

6.1 Fuzzy rules

Fuzzy control is suitable for multi-objective, nonlinear, time-varying systems and has wide applicability. This paper adopts the Mamdani-type fuzzy controller and uses "If..., then..." statements to establish fuzzy rules.

Since the driving and feedback states have different logic, each strategy is established individually. The input variables of the fuzzy policy-driven state are SOC_b, SOC_u, and P_{dri}, and the input variables of the feedback state are SOC_b, SOC_u, and P_{re}. The domain of discourse of SOC_b is from 0.2 to 1; the domain of discourse of SOC_u is from 0.4 to 1, and the fuzzy subsets are divided into L, M, and H, representing low, medium, and high. The domains of discourse of P_{dri} and P_{re} are both from 0 to 1, and the fuzzy subsets are divided into SL, L, M, H, and SH—extremely low, low, medium, high, and extremely high. The membership functions of SOC_b, SOC_u, and P_{dri} are shown in Fig. 14.

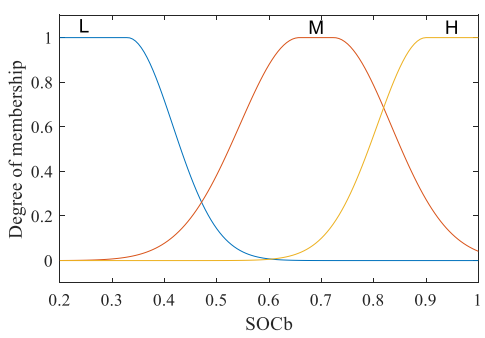

(a) The membership functions of SOC_b

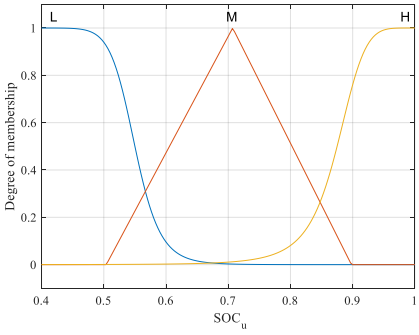

(b) The membership functions of SOC_u

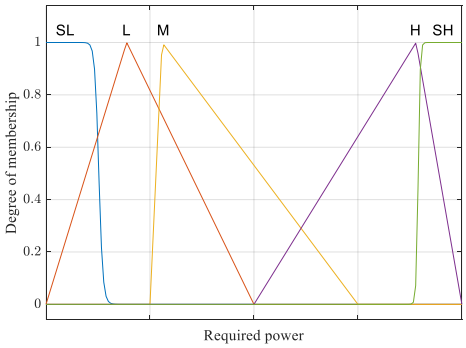

(c) The membership functions of P_{dri}

Figure 14. Membership functions of driving status inputs.

The output gain coefficient is the proportionality coefficient of the ultracapacitor in the required power; its universe of discourse is from 0 to 1; and the fuzzy subset is divided into SL, L, M, H, and SH (extremely low, low, medium, high, extremely high). The membership function rule is: When the battery is sufficiently charged, the ultracapacitor and the battery work together, reducing the charge and discharge current of the battery when the power demand is high, and avoiding the charging and discharging of the ultracapacitor and DC-DC when the power demand is low. When the SOC_b is low, the energy feedback to the battery is given priority. The rules are shown in Tables 3 and 4. We refer to the fuzzy control strategy as FZY-EMS in this work.

Table 3. Driving state fuzzy control rules

P_{dri}	SOC_b∈L			SOC_b∈M			SOC_b∈H		
	SOC_u			SOC_u			SOC_u		
	L	M	H	L	M	H	L	M	H
SL	SL	SL	SL	SL	SL	SL	SL	SL	SL
L	SL	SL	SL	SL	SL	SL	L	L	L
M	SL	M	H	SL	L	H	L	M	H
H	L	M	H	SL	M	H	L	H	H

SH	L	H	SH	L	H	SH	SL	H	SH

Table 4. Energy recovery fuzzy control rules

P_{re}	$SOC_b \in L$			$SOC_b \in M$			$SOC_b \in H$		
	SOC_u			SOC_u			SOC_u		
	L	M	H	L	M	H	L	M	H
SL	SL	SL	SL	ML	SL	SL	M	SL	SL
L	SL	SL	SL	SH	M	SL	SL	SH	SH
M	SL	SL	SL	SH	M	L	SH	H	M
H	SL	SL	SL	SH	M	L	SH	SH	M
SH	SL	SL	SL	SH	M	SL	SH	SH	M

6.2 PSO algorithm to optimize fuzzy strategy

The membership function of the above fuzzy control strategy depends on the subjective experience of experts, so the rules may not be optimal. In this paper, particle swarm optimization (PSO) is used to optimize the fuzzy control. The objective function when the weight coefficient is 0.47 is iterated, and the optimized membership function is applied to the energy distribution of the composite power system. The fuzzy strategy subjected to particle swarm optimization is called PFZY-EMS in this work.

Theoretically, the more parameters that the particle swarm optimization algorithm optimizes, the more chance it has to achieve the globally optimal solution. However, as the number of parameters increases, the particle swarm rules and the number of iterations increase, which will eventually lead to a substantial increase in computation time. We maintain the original fuzzy rules; the membership function of the rule boundary is removed by PSO optimization.

First, the parameters to be optimized are uniformly encoded. When the boundary of P_{dri} is removed, the membership parameters to be optimized are recorded as P_{dri1}, P_{dri2}, … and P_{dri11}. When the SOC_u boundary is removed, the membership parameters to be optimized are recorded as SOC_{u1}, SOC_{u2}, SOC_{u3}, and SOC_{u4}. When the SOC_b boundary is removed, the membership parameters to be optimized are recorded as SOC_{b1}, SOC_{b2}, SOC_{b3}, and SOC_{b4}, while the membership parameters to be optimized for P_{re} are recorded as P_{re1}, P_{re2}, … and P_{re11}. So there are 38 parameters that need to be optimized.

The steps to optimize fuzzy rule parameters using PSO are as follows:

Step 1: Take optimization variables X = (P_{dri} ,P_{dri2} ,..., P_{dri11}, SOC_{u1}, SOC_{u2}, ..., SOC_{u4}, SOC_{b1}, SOC_{b2}, ..., SOC_{b4}, P_{re1}, P_{re2}..., P_{re11}) as particles. Each dimension is encoded with real numbers, and the position and velocity of each particle are randomly initialized within their respective ranges.

Step 2: Decode each particle, output it to the fuzzy control rule as the corresponding membership parameter, and simulate the constructed pure electric vehicle model.

Step 3: Update the particle position and velocity by evaluating the current optimal position and the optimal position of the entire particle swarm using these equations:

$$v_i^{t'} = wv_i^{t'-1} + c_1 rand()(pbest_i^{t'-1} - x_i^{t'-1}) + c_2 rand()(gbest_i^{t'-1} - x_i^{t'-1}) \tag{19}$$

$$x_i^{t'} = x_i^{t'-1} + v_i^{t'-1} \tag{20}$$

where w is the inertia factor, v_i is the particle speed, x_i is the current position of the particle, $rand()$ is a random number between 0 and 1. c_1 and c_2 are learning factors (with $c_1 = c_2 = 2$ in this study), and i and t' are the particle number and the number of iterations, respectively.

Step 4: Return to Step 3 to iterate until the number of iterations does not change for 400 consecutive generations, and use g_{best} as the optimal parameter of the fuzzy control rule.

The drive state input membership function optimized by PSO is shown in Figure 15.

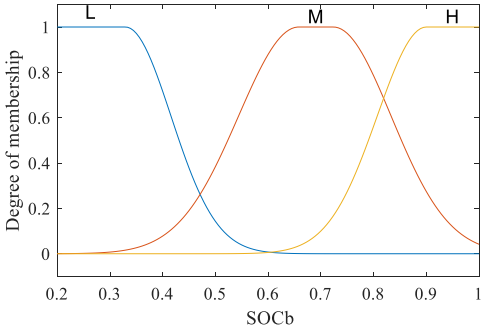

(a) Membership functions of SOC_b

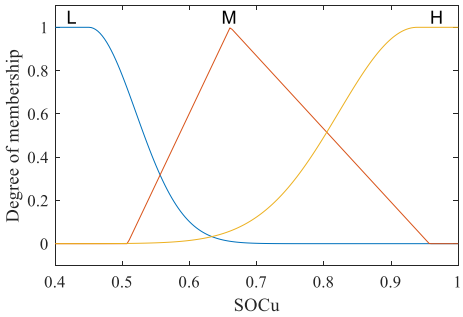

(b) Membership functions of SOC_u

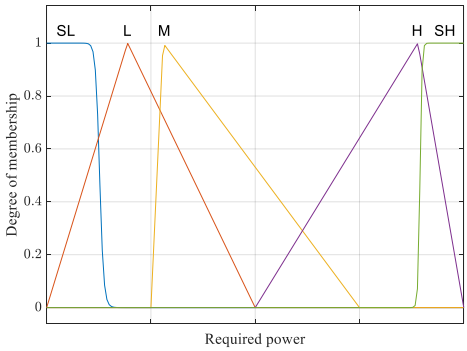

(c) Membership functions of P_{dri}

Figure 15. Membership functions of driving state inputs after PSO optimization.

7. RESULTS AND ANALYSIS

Taking WLTP and synthesis driving cycles as examples, the fuzzy energy management strategy based on particle swarm optimization is analyzed and compared with fuzzy control and energy management strategies based on DP. The simulation results are shown in Figures 16 and 17.

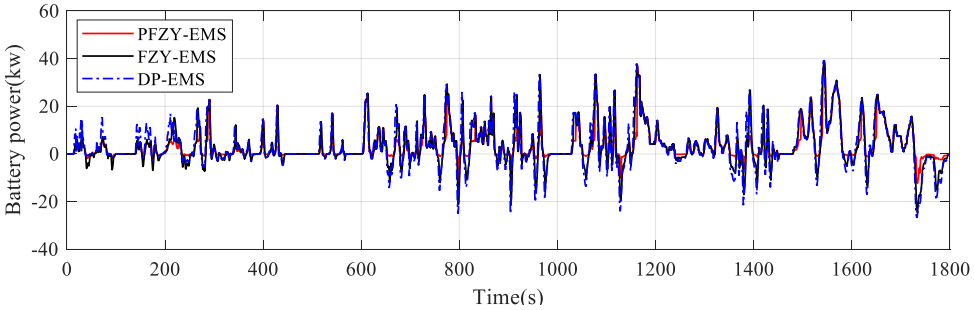

(a) For the WLTP driving cycle.

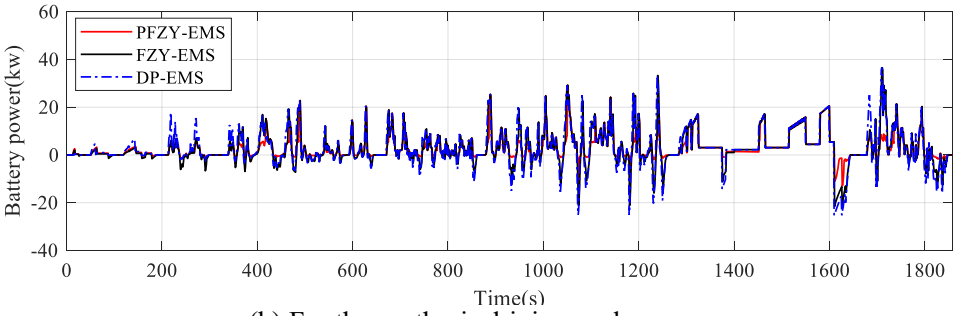

(b) For the synthesis driving cycle.

Figure 16. Battery power of the different EMSs.

Fig. 16 shows the output power of the battery for three energy management strategies for two driving cycles. It can be seen that the energy management strategy of particle swarm optimization fuzzy control proposed in this paper effectively avoids high current charge and discharge of the battery pack, which slows the aging process of the battery pack, and is closer to the energy management curve based on DP.

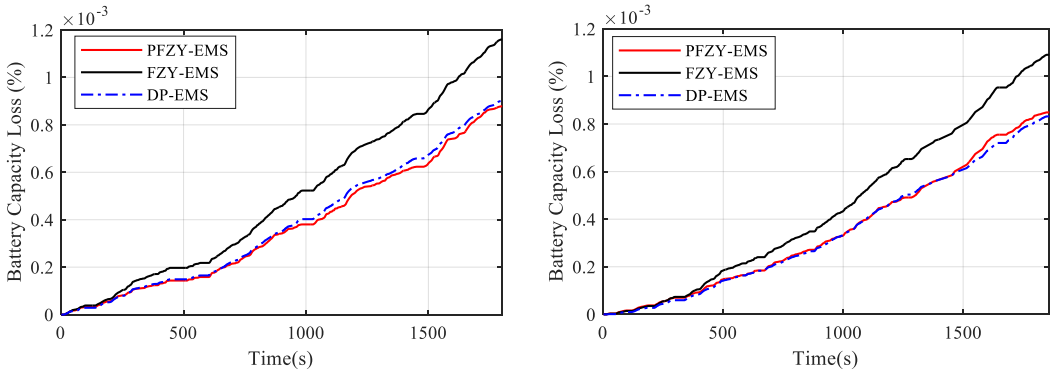

(a) Capacity loss of the battery.

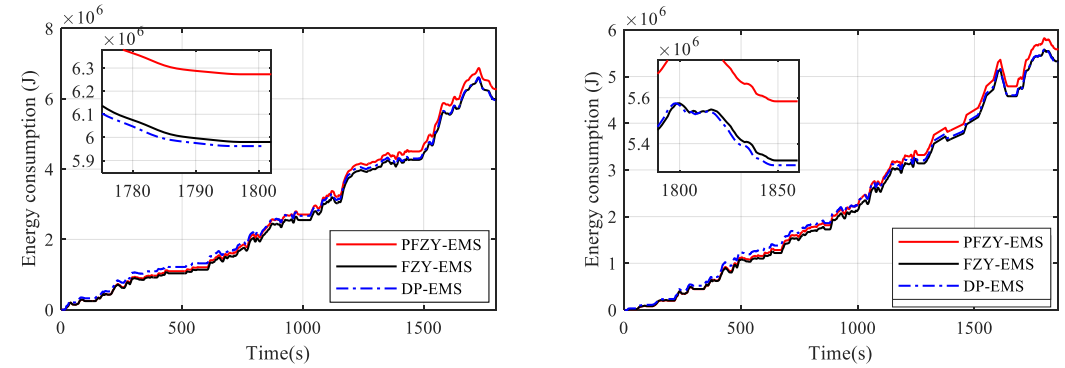

(b) Energy consumption.

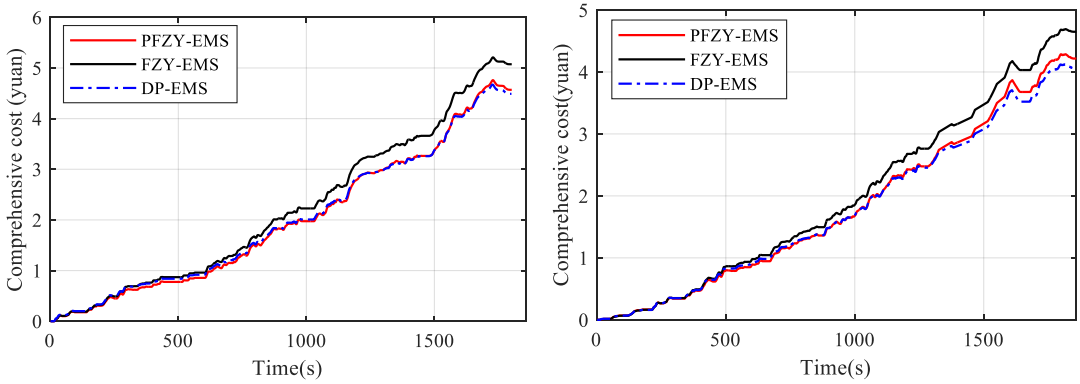

(c) Comprehensive cost.

Fig.17 Simulation results of the three EMSs under the two driving cycles. For each part, results for the WTLP cycle are on the left and for the synthesis cycle on the right.

Fig. 17 compares the simulation results of the three energy management strategies PFZY-EMS, FZY-EMS, and DP-EMS for two driving cycles.

Fig. 17 (a) shows the battery capacity loss as a function of time. For the WTLP cycle, the battery capacity loss for PFZY-EMS lies initially (0 to 680 s) between the losses for DP-EMS and FZY-EMS, closer to DP-EMS. From 681 s to the end of the cycle, the battery capacity loss for the PFZY cycle is the least. For the synthesis cycle, the capacity loss of PFZY-EMS battery is much lower than that of FZY-EMS and slightly higher than that of DP-EMS. At the end of the cycle, under the WLTP cycle, the battery capacity losses of the three strategies were 0.878×10^{-3} for PFZY-EMS, 1.161×10^{-3} for FZY-EMS, and 0.9×10^{-3} for DP-EMS. For the synthesis cycle, the battery capacity losses of these three strategies were 0.849×10^{-3}, 1.091×10^{-3}, and 0.832×10^{-3}, respectively. For this cycle, the PFZY-based strategy outperforms the FZY strategy and is slightly inferior to the DP strategy.

Figure 17(b) shows the energy consumption trends of these three systems—PFZY-EMS, FZY-EMS, and DP-EMS—for the two driving cycles. The graphs show that: for the WLTP cycle, the system energy consumption of the PFZY-EMS strategy is between those of DP-EMS and FZY-EMS from the start of the vehicle operation to 928 s, and that from 929 s to the end of the cycle, the system energy consumption for the PFZY-EMS strategy is higher than for the other two strategies. For the synthesis cycle, the system energy consumption of the PFZY-EMS strategy is between those of DP-EMS and FZY-EMS from 0 to 1068 s, and from

1069s to the end of the cycle, its system energy consumption is the greatest. At the end of the cycle, under the WLTP cycle, the energy consumptions of the three strategies are 6.273×10^6, 5.98×10^6, and 5.962×10^6 J, respectively; under the synthesis cycle, the cycle energy consumptions of the three strategies are, respectively, 5.584×10^6, 5.327×10^6, and 5.036×10^6 J.

Figure 17(c) shows the comprehensive cost trends of the of PFZY-EMS, FZY-EMS, and DP-EMS strategies for two driving cycles. At the end of the WLTP cycle, the comprehensive costs of the three strategies are 4.569, 5.074, and 4.490 yuan, respectively. At the end of the synthesis cycle, the cycle energy consumption of the three strategies are 4.217, 4.649, and 4.063 yuan, respectively. The cycle energy consumption of the PFZY strategy is higher than those of the other two strategies. The reason is that the optimization objective function in this work is the comprehensive cost, and the battery aging cost is much higher than the energy consumption cost. The energy management strategy proposed here greatly reduces the capacity loss of the power battery and the comprehensive cost of the composite power supply at a small energy consumption cost.

The numerical results are shown in Table 5. Compared with FZY-EMS, the energy management strategy proposed in this paper reduces the battery capacity loss by 24.374% and 22.181%, and the system energy consumption increases by 4.900% and 4.824%, respectively. Comprehensive costs were reduced by 9.953% and 9.292%, respectively. Compared with DP-EMS, the battery capacity loss is reduced by 24.374% under the WLTP cycle, and the battery capacity loss is increased by 2.043% under the synthesis cycle, the system energy consumption is increased by 5.216% and 10.882%, respectively. The comprehensive cost increased by 1.759% and 3.790% respectively. The results show that the PSO-optimized fuzzy energy management strategy is much higher than the fuzzy control strategy and slightly lower than the dynamic programming strategy, and has significant benefits.

Table 5. Comparison of evaluation indicators.

Strategy	Battery capacity loss (%)		Energy consumption (10^6 J)		Comprehensive cost (yuan)	
	WLTP	Synthesis	WLTP	Synthesis	WLTP	Synthesis
PFZY-EMS	0.878	0.849	6.273	5.584	4.569	4.217
FZY-EMS	1.161	1.091	5.980	5.327	5.074	4.649
DP-EMS	0.900	0.832	5.962	5.036	4.490	4.063

8. CONCLUSIONS

The energy management of electric vehicles with a hybrid energy storage system was studied in this work. The weighted sum of the battery capacity loss and energy consumption under sample driving cycles were taken to minimize the objective function, and the objective function was then solved by dynamic programming. The

objective function value under the weight coefficient was obtained, and the corresponding composite power distribution relationship and the comprehensive cost composed of battery aging cost and power consumption cost were obtained. Based on these optimization results, the particle swarm algorithm was used to optimize fuzzy logic membership parameters, and a real-time fuzzy energy management strategy was developed. The fuzzy strategy based on particle swarm optimization, fuzzy control strategy, and energy management strategy based on dynamic programming (DP) were compared and analyzed in the research cycle and the verification cycle. The results show that the energy management strategy proposed in this work is effective.

This energy management strategy has not been verified in actual vehicles. In follow-up work, a test system will be built to conduct performance tests, and the strategy will be continuously optimized according to the test results.

REFERENCES:

[1] B. Zhao, Q. Song, and W. Liu, "Power characterization of isolated bidirectional dual-active-bridge DC-DC converter with dual-phase-shift control," *Power Electronics, IEEE Transaction on*, vol.27, pp.4172-4176, Sept. 2012.

[2] C.-X. Song, F. Zhou, and F. Xiao, "Energy management optimization of Hybrid Energy Storage System(HESS) based on dynamic programming,"*Journal of Jilin University* (*Engineering and Technology Edition*) , pp. 8-14, Jan. 2017.

[3] T.-Z. Yao, C.-J. Xie, T. Zeng, and L. Huang, "Multi-Fuzzy control based energy management strategy of battery / super-capacitor hybrid energy system of electric vehicles," *Automotive Engineering*, pp. 615-640, Jun.2019.

[4] Z.-Y. SONG, "The optimization and control of li-battery/supercapacitor hybrid energy storage system for bus," *Beijing: Tsinghua University*, 2016.

[5] D. Xu , H. Zhou , B. Wang , "A simplified cascading hybrid power and its control scheme for electric vehicles," *Automotive Engineering*, pp. 1368-1374, Oct. 2017.

[6] Y.-T. Luo , and X.-T. Liu , "Design on extended storage life of li-ion batteries of composite power system for electric vehicles," *Journal of South China University of Technology (Natural Science Edition)* , pp. 51-59, Mar. 2016.

[7] M. Ding , G. Lin , and Z.-N. Chen , "A control strategy for hybrid energy storage systems," *Proceeding of the CSEE*, vol 32, pp. 1-6, Feb. 2012.

[8] J.-J. Hu , Y. Zhang , Z.-H. Hu , and J. Xiao, "Parameter matching and control strategies of hybrid energy storage system for pure electric vehicle," *China Journal of Highway and Transport*, pp. 142-150, Mar. 2018.

[9] J. Li , Y.-Z. Zhu , L. Ji , and Y.-J. Xu, "Optimization of fuzzy control strategy for hybrid electric vehicle," *Automotive Engineering*, pp. 10-14, Jan. 2016.

[10] S. Du , and C.-C. Zuo , "Self-adaptive fuzzy PI control in energy distribution of pure electric vehicle with dual-energy storage," *International Journal of Control & Automation*, pp. 283-298, Jul. 2014.

[11] Y.-H. Li , X.-M. Lu , and C. Narayan , "Rule-based control strategy with novel parameters optimization using NSGA-II for power-split PHEV operation cost minimization," *IEEE Transactions on Vehicular Technology*, vol. 63, pp. 3051-3061, Jul. 2014.

[12] Y.-H. Cheng , and C.-M. Lai, "Control strategy optimization for parallel hybrid electric vehicles using a memetic algorithm," *Energies*, vol.3, pp. 305-326, Oct. 2017.

[13] X.-S. Hu, N. Murgovki, L.-M. Johannesson, and B. Egardt, "Comparison of three electrochemical energy buffers applied to a hybrid bus powertrain with simultaneous optimal sizing and energy management," *IEEE Transactions on Intelligent Transportation Systems*, vol. 15, pp. 1193-1205, Mar. 2014.

[14] F. Zhou, C.-X. Song , T.-W. Liang, and F. Xiao, "Parameter Matching of on-board Hybrid Energy Storage System Using NSGA-II Algorithm," *Journal of Jilin University (Engineering and Technology Edition)*, pp. 1336-1343, Sept. 2017.

[15] Z. -Y. Song, J.-Q. Li, X.-B. Han, X.-W. Zhang, M. Gao, and O. Yang, "A comparison study of different semi-active hybrid energy storage system topologies for electric vehicles," *Journal*

of Power Sources, vol. 274, pp. 400-411, 2015.
[16] Z-Y CHEN,R XIONG and J-Y CAO."Particle swarm optimization-based optimal power management of plug-in hybrid electric vehicles considering uncertain driving cycles",*Energy* , pp. 197-208, Jan. 2016.
[17] S-B XIE,K-K ZHANG, Q-K ZHANG and H-R LUO."Study on energy management strategy for parallel plug-in hybrid electric vehicles considering battery electric-thermal-depth-of-discharge", *Automotive Engineering* ,vol.43, pp. 791-798, June. 2021.
[18] P. Zhang, F.-W. Yan, and C.-Q. Du, "A comprehensive analysis of energy management strategies for hybrid electric vehicle based on bibliometrics," *Renewable and sustainable energy reviews*, vol. 48, pp. 88-104, 2015.
[19] L. Zhang, X.-S. Hu, Z.-P. Wang, F.-C. Sun, J.-J. Deng, and D.-G. Dorrell, "Multi-objective optimal sizing of hybrid energy storage system for electric vehicles," *IEEE Transactions on Vehicular Technology*, pp.1, 2017.
[20] X. Wu, X. Yan, Y. Wang, B.-X. Huang, and Z.-C. Liu, "Study on DC resistance characteristics of ternary lithium batteries," *Chinese Journal of Power Sources*, pp. 568-684, Apr. 2019.
[21] D.-T. Qin, Z.-Y. Peng, Y.-G. Liu, "Dynamic Energy Management Strategy of HEV Based on Driving Pattern Recognition," *China Academic Journal Electric*, pp. 1550-1555, Jun. 2014.
[22] S. Masoud, and Y.-K. Tare, "Multi-objective optimal design of hybrid renewable energy systems using PSO-simulation based approach," *Renewable Energy*, pp. 67-79, 2014.
[23] L.-H. Xi, X. Zhang, and C. Geng, "Energy management strategy optimization of extended-range electric vehicle based on dynamic programming," *Journal of Traffic and Transportation Engineering*, pp. 148-156, Jun. 2018.
[24] S.-B. Xie, T. Liu, H.-L. Li, and Z.-K. Xin, "A study on predictive energy management strategy for a plug-in hybrid electric bus based on Markov Chain," *Automotive Engineering*, pp. 871-877, Aug. 2018.